

Towards 100% renewable energy systems: The role of hydrogen and batteries

Original

Towards 100% renewable energy systems: The role of hydrogen and batteries / Marocco, Paolo; Novo, Riccardo; Lanzini, Andrea; Mattiazzo, Giuliana; Santarelli, Massimo. - In: JOURNAL OF ENERGY STORAGE. - ISSN 2352-152X. - 57:(2023), p. 106306. [10.1016/j.est.2022.106306]

Availability:

This version is available at: 11583/2973792 since: 2022-12-13T11:08:33Z

Publisher:

Elsevier

Published

DOI:10.1016/j.est.2022.106306

Terms of use:

This article is made available under terms and conditions as specified in the corresponding bibliographic description in the repository

Publisher copyright

Elsevier postprint/Author's Accepted Manuscript

© 2023. This manuscript version is made available under the CC-BY-NC-ND 4.0 license
<http://creativecommons.org/licenses/by-nc-nd/4.0/>. The final authenticated version is available online at:
<http://dx.doi.org/10.1016/j.est.2022.106306>

(Article begins on next page)

Towards 100% renewable energy systems: the role of hydrogen and batteries

Paolo Marocco^{*1}, Riccardo Novo^{2,3,4}, Andrea Lanzini^{1,4}, Giuliana Mattiazzo^{2,3,4},
Massimo Santarelli^{1,5}

¹Dipartimento Energia "Galileo Ferraris", Politecnico di Torino, 10129, Torino,
Italy

²Dipartimento di Ingegneria Meccanica e Aerospaziale, Politecnico di Torino,
10129, Torino, Italy

³MOREnergy Lab, Politecnico di Torino, 10129, Torino, Italy

⁴Energy Center Lab, Politecnico di Torino, 10129, Torino, Italy

⁵CO₂ Circle Lab, Politecnico di Torino, 10129, Torino, Italy

*Corresponding author: paolo.marocco@polito.it

Abstract

New challenges arise for the accurate modelling of energy systems with a high share of renewable energy. In this context, energy storage technologies become key elements to manage fluctuations in renewable energy sources and electricity demand. The aim of this work is to investigate the role of batteries and hydrogen storage in achieving a 100% renewable energy system. First, the impact of time series clustering on the multi-year planning of energy systems that rely heavily on energy storage is assessed. The results show good accuracy, even for a small number of representative days, which is necessary to limit the computational burden of the optimisation problem. Then, different configurations of carbon-free energy systems are considered by varying the energy storage solution: only-battery, only-hydrogen, and hybrid scenarios. An island energy system based on photovoltaics and floating offshore wind turbines is used as a demonstrative case study. It is shown that the cost of the only-battery configuration is 155% higher than the cost of the hydrogen-based scenarios. The reason is that the long-term hydrogen-based storage, despite its low round-trip efficiency, avoids costly oversizing of batteries and wind turbines throughout the analysed period. In the selected

33 case study, hydrogen storage reduces the total rated power of the wind farm by about 5
34 times compared to the only-battery system. Hydrogen-based solutions are therefore
35 crucial in 100% renewable energy systems to achieve energy self-sufficiency in a cost-
36 effective way.

37 **Keywords**

38 Renewable energy systems; Renewable energy sources; Hydrogen; Battery;
39 Energy storage; Energy modelling

40 **1 Introduction**

41 In recent years, there has been growing interest in developing sustainable energy
42 systems based on renewable energy sources (RESs). The deployment of RESs at a large
43 scale is the first step in the transition to a low-carbon economy. However, the fluctuating
44 behaviour of variable RESs, e.g., wind and solar, leads to new challenges in terms of
45 electric grid management and energy storage. The installed capacity of electrical energy
46 storage (EES) systems is thus expected to increase significantly in the coming years.
47 Energy storage solutions can be of different types: mechanical, electrochemical,
48 chemical, electrical and thermal [1,2]. Batteries offer high efficiency and fast response
49 time [3], making them ideal candidates when small size and short-term energy storage is
50 needed. Hydrogen is also expected to become essential as a storage solution in RES-
51 based scenarios due to its long-term storage capability and high energy density [4].
52 Hydrogen can be generated in a sustainable way through water electrolysis powered by
53 renewable energy [5]. Once hydrogen is produced, it can be stored and later reconverted
54 into electricity according to the so-called power-to-power (PtP) route. Moreover, and
55 differently from a closed battery (pure role of electrical storage), hydrogen can assume
56 other roles: as feedstock for production of gaseous and liquid synthetic chemicals via
57 dedicated power-to-X (PtX) routes in a cross-sector perspective [6]. As highlighted by
58 Lund *et al.* [7], an integrated cross-sector approach can promote a large penetration of
59 renewable energy sources, by providing additional flexibility in the energy system. In this
60 context, the potential integration of the electricity, heat, transport and industrial sectors -
61 as part of a smart energy system - has been shown to be beneficial in achieving 100%
62 renewable energy supply [8]. Indeed, sector coupling can mitigate the need for grid
63 expansion and storage capacity [9].

64 In islands, diesel generators (DGs) are still the most widespread choice for
65 electricity production [10,11]. Local RESs can represent an effective solution to mitigate
66 DG-related pollution problems and reduce the cost of electricity [12]. However, the
67 adoption of EES solutions is crucial to improve the RES exploitation and enhance the
68 reliability of the power supply service. Accurate sizing of the energy storage is thus
69 necessary when dealing with hybrid renewable energy systems (HRESs) for stand-alone
70 applications [13]. In this context, in the literature, increasing attention has recently been
71 paid to the optimal design of stand-alone HRESs to minimise the system cost while
72 keeping the energy provision reliable and less polluting [14]. As reported in the review by
73 Liu *et al.* [15], the combination of PV, wind, diesel, and batteries was proven to be feasible,
74 cost-effective, and with a low environmental impact. Prina *et al.* [16] showed that the cost
75 of energy supply increases exponentially as the share of variable RESs increases; the
76 most challenging and expensive phase of the energy transition is from 70% to 100% of
77 the RES share. High-RES penetration, indeed, entails the oversizing of the HRES
78 components, with consequent sharp rise in the cost of energy [17]. In this context, the
79 use of hydrogen was found to be effective in limiting the cost increase when pursuing full-
80 RES system configurations in off-grid insular communities [18]. The hybridisation of
81 batteries with hydrogen can represent a cost-effective choice when relying on local RESs
82 in isolated areas [19]. A 35% cost reduction was reported for the hybrid hydrogen-battery
83 configuration compared to the only-battery system in a 100% RES-based scenario [20].

84 As shown in the review article by Chang *et al.* [21], there is a wide range of tools
85 for modelling energy systems: from commercially available software, to open-access
86 modelling frameworks, and in-house proprietary tools. Current research trends seek to
87 address cross-sector synergies and improved temporal detail, with an increasing focus
88 on open-access models. Several modelling methods have been used to investigate the
89 decarbonisation of islands. HOMER is a well-known commercial software mainly used for
90 the optimal sizing of RES-based energy systems at the micro-grid level. It can combine
91 many components and perform optimisation and sensitivity analyses, which simplifies the
92 evaluation of the most favourable system configuration [22,23]. Metaheuristic-based
93 models are also widely employed for micro-grid applications to perform the optimal design
94 of HRESs [24]. When dealing with the energy planning at the whole-island level,
95 established modelling frameworks include EnergyPLAN, TIMES and OSeMOSYS [25].
96 They were originally designed for applications at the country level, but have been applied

97 extensively at the island level as well [15]. These tools typically use the linear
98 programming (LP) or mixed integer linear programming (MILP) techniques to solve the
99 energy planning problem. TIMES [26] and OSeMOSYS [27] are based on a multi-year
100 time horizon approach, which allows overcoming intrinsic problems associated with a
101 single-year formulation. Indeed, the single-year-based framework cannot describe
102 important phenomena, such as an increase in energy demand over the project lifetime,
103 changes in long-term behaviour of RESs and changes in the cost of technologies over
104 time. However, in multi-year capacity expansion models, time series must be
105 approximated to reduce the computational burden of the simulation. Each year is
106 generally divided into time slices, which are identified by a season, a day type (i.e., day
107 of a season) and a daily time bracket (i.e., fraction of the day) [28]. Increasing the number
108 of time slices improves the accuracy of the time series representation, but at the expense
109 of a more complex problem. The study of scenarios with high RES penetration, and the
110 consequent introduction of EES solutions in energy systems, makes the correct
111 representation of time series even more important [29]. Novo *et al.* [30] addressed this
112 issue by investigating techniques to reduce the number of time slices and limit the
113 computational time when dealing with multi-year energy system models. In particular,
114 they evaluated the advantages of time series clustering and showed good accuracy of
115 results when only a few representative days (RDs) are used. The benefits of
116 representative days have also been demonstrated in other works, where a single-year
117 modelling approach has been adopted [31–33]. Gabrielli *et al.* [31] pointed out that the
118 interconnection of RDs (based on the chronological order of days over the year) is
119 necessary to accurately model multi-energy systems with seasonal energy storage [31].
120 Consistent with this finding, Kotzur *et al.* [32] showed that uncoupled representative
121 periods are not suitable for modelling energy systems based on high-capacity energy
122 storage. Hoffmann *et al.* [33] reported that the optimal choice of aggregation methods
123 depends on the mathematical structure of the energy system optimisation model. They
124 also showed that the use of representative days is the Pareto-optimal aggregation
125 approach when storage is considered.

126 This work assesses the impact of time series clustering in the long-term planning
127 of energy systems, making use of interconnected clustered representative days.
128 OSeMOSYS, an open-source multi-year modelling framework, was employed in the
129 present study, further investigating the methodology introduced in [30]. Specifically, a

130 comparative assessment of the traditional and updated OSeMOSYS versions was
131 conducted to evaluate the effectiveness of the proposed methodology to model the multi-
132 year evolution of renewable-based energy systems that rely heavily on energy storage.
133 The island of Pantelleria (in southern Italy) was considered as a demonstrative case study
134 for this analysis. A relatively simple reference energy system was used to better highlight
135 the impact of interconnected clustered RDs in modelling long-term energy storage. Then,
136 different configurations of carbon-free power systems were analysed by varying the EES
137 solution to shed light on the role of batteries and hydrogen in achieving 100% renewable
138 energy systems. Specifically, the only-battery, only-hydrogen, and hybrid (i.e., battery
139 plus hydrogen) configurations were examined.

140 The structure of this work is the following: Section 2 describes the methodology
141 that has been developed for the energy system modelling. This section also presents the
142 selected case study and the various scenarios that will be investigated. The main results
143 are then shown and discussed in Section 3, and finally, the key conclusions are summed
144 up in Section 4.

145 **2 Materials and methods**

146 This section depicts the overall methodology implemented in this paper to explore
147 the future role of batteries and hydrogen in energy systems with a high share of renewable
148 energy. First, the modelling framework used is depicted. Then, the model of the insular
149 energy system is presented along with the main techno-economic assumptions. Finally,
150 the strategy identified for the development of different energy scenarios is described.

151 **2.1 Modelling framework**

152 The energy model has been developed using OSeMOSYS, an LP-/MILP-based,
153 open-source, multi-year energy modelling framework [27]. In this work, both the
154 conventional OSeMOSYS version [34] and the enhanced version presented by Novo *et*
155 *al.* [30] were used. For both versions, an additional set of equations was introduced to
156 enable a discussion about the storage systems analysed in this article.

157 The structure of OSeMOSYS is based on the following elements: sets, which
158 determine the model structure; parameters, which are the model inputs; variables, which
159 are the outputs of the model; and equations, which relate parameters and variables. Each
160 parameter and variable is a function of one or more sets.

161 The physical model structure is based on the following sets: *regions*, which are
 162 areas where the balance between supply and demand is guaranteed; *fuels*, which are the
 163 energy commodities; *technologies*, which are the elements that transform, import or
 164 export *fuels*; and *storages*, which are used to store *fuels* between time intervals.

165 The objective function (OF) is to minimise the net present cost (NPC) of the energy
 166 system [35]. As shown in Eq. (1), OF is given by the sum of the discounted costs of all
 167 *technologies* (t) and *storages* (s) over all *regions* (r) and *years* (y). The discounted costs
 168 can include capital, fixed and variable terms.

169

$$OF = \min \left(\sum_r \sum_y \left(\sum_t TotalDiscountedCostByTechnology_{r,t,y} \right. \right. \\ \left. \left. + \sum_s TotalDiscountedStorageCost_{r,s,y} \right) \right) \quad (1)$$

170

171 where the $TotalDiscountedCostByTechnology_{r,t,y}$ is the total discounted cost of the t -
 172 th *technology* in the y -th year, and $TotalDiscountedStorageCost_{r,s,y}$ is the total discounted
 173 cost of the s -th *storage* in the y -th year.

174 The key decision variables are the annual installed capacity of *technologies* and
 175 *storages* in each year and the activity of *technologies* and *storages* (i.e., a measure of
 176 their operation) in each time interval.

177 2.1.1 TRAD method

178 The time representation in the common version of OSeMOSYS is the same as that
 179 of typical LP/MILP-based frameworks for long-term optimal expansion planning of energy
 180 systems [27]. It makes use of five sets: *years* (y), *seasons* (ls), *daytypes* (ld),
 181 *dailytimebrackets* (lh) and *timeslices* (l). Each modelled year consists of several *seasons*
 182 (e.g., spring, summer); *daytypes* (e.g., weekdays, weekends) recur in every *season*; and
 183 every *daytype* consists of several *dailytimebrackets* (e.g., morning, afternoon). The
 184 combination of a *season*, a *daytype*, and a *dailytimebracket* represents a *timeslice*. All
 185 time-related input profiles (e.g., power load profiles, variable RES capacity factors) are
 186 obtained by averaging original (e.g., hourly) time series. This process - which is performed
 187 based on how *seasons*, *daytypes* and *dailytimebrackets* recur over the year - is necessary
 188 to reduce the complexity of the problem and allow the resolution of multi-year optimal

189 planning problems [28]. Nevertheless, such a practice tends to flatten peaks and troughs,
190 favouring low-cost variable renewables and underestimating the total system cost [36].
191 Especially, this conventional approach (named TRAD from now on) may lead to a weak
192 dimensioning of energy storage systems [37].

193 Accurate representation of energy storage becomes increasingly important as the
194 share of electricity from renewable sources increases. Concerning the energy storage
195 modelling, OSeMOSYS enables energy to be either stored or discharged during a
196 *timeslice* as long as the storage level remains within specified minimum and maximum
197 values. A timeline of *timeslices* is obtained by assigning each *timeslice* to a *season*, a
198 *daytype* and a *dailytimebracket*, which is needed for a correct modelling of the energy
199 storage. However, as discussed in [38], it is not necessary to verify that the storage levels
200 are within their boundaries at each time interval over the year. Indeed, based on the
201 TRAD time representation, extreme storage level values can only occur during the first
202 and last week of a specific *season*, and during the first and last occurrences of a particular
203 *daytype*.

204 **2.1.2 NEW method**

205 In this analysis we considered, and further investigated, the OSeMOSYS update
206 proposed by Novo *et al.* [30], where interconnected clustered representative days were
207 implemented to improve the modelling of energy systems with high RES share [39].

208 In contrast to TRAD, where sequential averaging of time series is performed, in
209 the NEW method representative days are defined using a clustering procedure based on
210 specific attributes, namely time series profiles of RES supply and electricity demand.

211 As displayed in Figure 1, the first step is to cluster the time series: the aim is to
212 merge all days of the year into a predefined number of groups (representative days) so
213 that the group members are as similar as possible. The clustering process was performed
214 through the k-means algorithm [32]. According to this technique, clusters are created by
215 minimising the squared error between the empirical mean of a cluster and all candidates
216 in the cluster. More specifically, it is minimised a distance measure of some attributes
217 between each group member. The major advantage related to the k-means method is
218 that the total value of the original time series is preserved for each attribute. In this work,
219 the following attributes were considered for the clustering: PV capacity factor, wind
220 capacity factor and electricity demand. At the end of the clustering procedure, each day
221 of the year is assigned to one of the representative days.

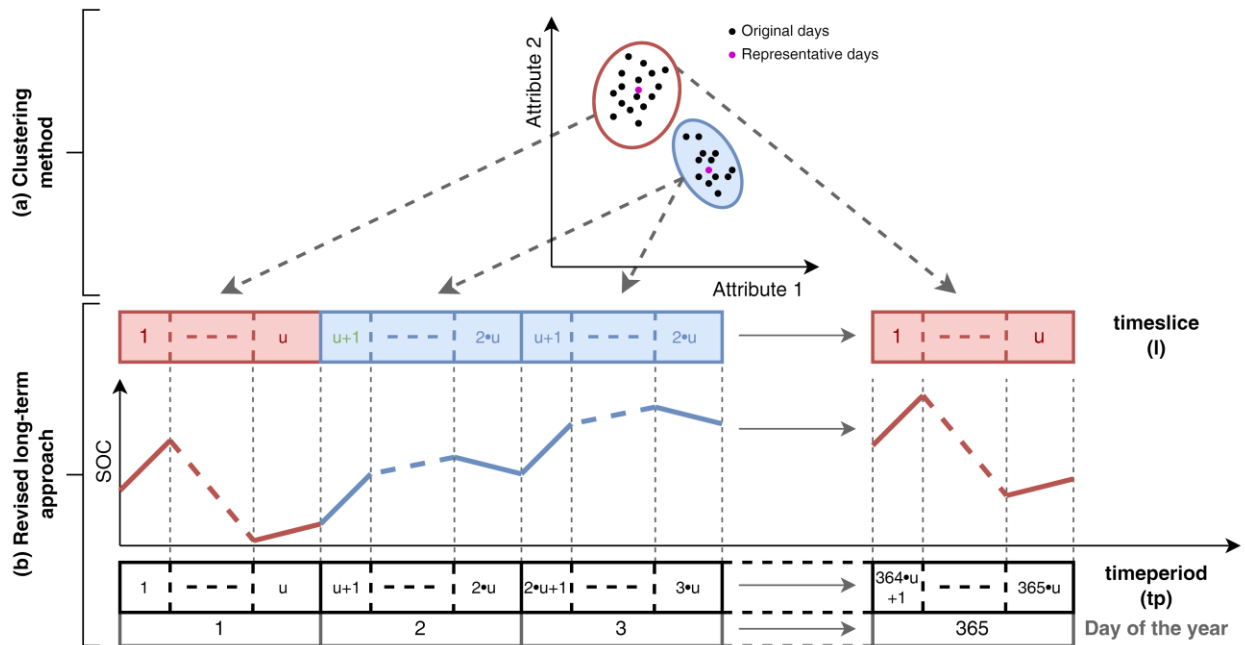
222 Figure 1 also shows that each day consists of a certain number (u) of time
223 intervals. Section 2.2 provides details on the accuracy that has been adopted for the
224 intraday variability (Table 2). The number of *timeslices* of the model is thus given by u
225 multiplied by the number of representative days.

226 The TRAD framework was then revised to allow the implementation of clustered
227 time series while considering the chronological order of the representative days (and thus
228 *timeslices*) throughout the year. This chronological sequence is necessary for the
229 modelling of the energy storage.

230 In particular, a new temporal set, called *timeperiod* (tp), was introduced to account
231 for the chronology of *timeslices* over the course of the year. The number of *timeperiods*
232 is equal to u (i.e., the time intervals of a day) multiplied by the number of days in a year.
233 Each *timeperiod* is assigned a *timeslice* on the basis of the RD associated with the day
234 of that *timeperiod*. The introduction of *timeperiods* eliminates the need for *seasons*,
235 *daytypes* and *dailytimebrackets*, which are required instead in the TRAD method.

236 As shown in Figure 1, the energy balance of the *storage*, and thus its State-Of-
237 Charge (SOC) variation, is always the same when a certain *timeslice* occurs in the year.
238 However, the SOC at the beginning of each *timeperiod* tp is evaluated based on the SOC
239 at the beginning of the previous *timeperiod* $tp-1$ and the SOC variation in the *timeslice*
240 associated with the *timeperiod* $tp-1$. This formulation allows successive time intervals of
241 the year to be interconnected and was introduced to model the *storages* and describe
242 their long-term operating cycles when dealing with clustered time series. It should be
243 noted that, unlike the TRAD method, it is necessary to verify that the storage level (i.e.,
244 SOC value) remains within the SOC limits for each time interval during the year.

245 A sensitivity analysis on the number of representative days must be performed to
246 assess a reasonable trade-off between accuracy and computational time.



247

248 *Figure 1 – NEW method: Temporal framework with interconnected clustered*
 249 *representative days (modified from [30]). For the sake of clarity, a clustering process with two*
 250 *attributes is shown in the figure. However, in this analysis the clustering was performed*
 251 *considering three attributes: PV and wind capacity factors, and electricity demand. This figure*
 252 *also refers to a clustering process with two representative days. SOC is the State-Of-Charge of*
 253 *the storage.*

254

255 This paper goes beyond the work developed in [30], assessing the suitability of
 256 NEW for an isolated, 100% renewable-based energy system with a hybrid hydrogen-
 257 battery storage. Moreover, it aims to evaluate the role of storage systems with different
 258 durations on a long-term scale. It should be marked that the rated power and rated energy
 259 of storage systems are sized separately in OSeMOSYS, with different costs associated
 260 to power-related components (which are modelled as *technologies*) and energy-related
 261 components (which are modelled as *storages*). While this approach performs well for a
 262 hydrogen-based PtP solution, it is not suitable for batteries. In fact, many electrochemical
 263 storage technologies (e.g., Li-ion batteries, NaS batteries) are characterised by a well-
 264 defined range of energy-to-power ratios. For these EES systems, OSeMOSYS (both
 265 TRAD and NEW methods) has been updated by introducing lower and upper bounds on
 266 the ratio between the energy size and the power size. The new parameters and storage
 267 equations, along with the modified OSeMOSYS code, are included in Section 3 of the
 268 Supplementary Material.

269 **2.2 Energy model**

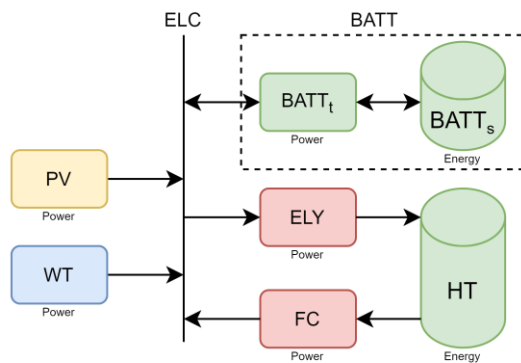
270 The island of Pantelleria was considered as a case study in this analysis. It is
271 located in the Strait of Sicily, south of Italy, and is not electrically connected to the
272 mainland. This medium-sized island is a good example of several other insular locations
273 across the Mediterranean area and thus represents a valuable case study to investigate
274 solutions for local energy self-sufficiency of remote sites [28].

275 The reference energy system of Pantelleria used in this work is displayed in Figure
276 2. It includes one *fuel*, five *technologies* and two *storages*. A *storage* set and at least one
277 *technology* set are needed to model a storage system in OSeMOSYS. *Technologies* are,
278 indeed, associated to a certain *storage* to enable its charging and discharging.

279 Electricity (ELC) is the *fuel*, which has an associated final demand. The
280 *technologies* are the following: photovoltaic power plants (PV), floating offshore wind
281 turbines (WT), electrolyser (ELY), fuel cell (FC), and battery technology (BATT_t). Two
282 different *storages* were considered: the hydrogen tank (HT) and the battery storage
283 (BATT_s). The ELY and FC are needed, respectively, to charge and discharge the
284 hydrogen tank. Analogously, the BATT_t technology was included for the
285 charging/discharging of the BATT_s storage.

286 Proton-Exchange Membrane (PEM) electrolysers were considered for hydrogen
287 production because of their excellent dynamic behaviour, making them suitable for
288 coupling with variable RESs [40]. The PEM typology was also chosen for the fuel cell
289 component. As for the BATT component, Li-ion batteries were considered because of
290 their high roundtrip efficiency, low self-discharge rate and wide cycling modulation range
291 [18]. Pressurised vessels were assumed for the hydrogen storage tank.

292



293

294

Figure 2 - Reference energy system of the analysed case study.

295
296 The investigation of renewables-based future energy scenarios requires an
297 accurate definition of the installable power limits of different technologies. A precise
298 estimate can be very challenging at a national level; nevertheless, it is more practicable
299 at the scale of a small island. The PV technical potential for the island of Pantelleria
300 amounts to 10.8 MW [28]. Such value was obtained as a sum of the 6 MW ground-
301 mounted PV potential established by the local municipality based on available land, and
302 the 4.8 MW rooftop PV potential, which would be reached with an average per-capita
303 installed capacity of around 0.60 kW_{PV}/person. Concerning wind power, the installation of
304 onshore wind turbines of any size is currently forbidden by the Sicilian regional law [41].
305 Although public authorities are currently engaged in a discussion on the topic, it was
306 assumed that the current legislative framework is not modified in this analysis. Therefore,
307 exclusively offshore wind turbines were considered. In addition, because of the very high
308 depths that characterise the sea in the Strait of Sicily, offshore wind turbines were
309 supposed to be installed on floating platforms, with a significant increase in the overall
310 cost of wind power. Specifically, floating wind turbines with a rated power of 2 MW each
311 were considered in this work.

312 The annual electrical demand in Pantelleria amounted to approximately 27.3 GWh
313 in 2021, with a power peak of 10.5 MW in the summer period due to tourism. It has been
314 assumed that the electrical load has an annual increase of 1.5%, mainly because of the
315 introduction of electric vehicles [28]. A seasonal behaviour is also present in the RES
316 production profiles: PV (annual production of 1610 kWh/kW) has a peak in the summer
317 period, whereas floating offshore wind (annual production of 3580 kWh/kW) is
318 characterised by greater productivity in the winter months, from around January to March.
319 The strong intra-annual variability of both RES supply and electrical demand profiles
320 suggests that energy storage systems are necessary to optimise the exploitation of local
321 RESs and, thus, achieve higher levels of renewable penetration.

322 Table 1 summarises the main techno-economic assumptions to estimate the
323 CAPEX and replacement costs of the components involved in the Pantelleria energy
324 system. The values of the operational life are also shown to know when replacements
325 take place. Cost projections were used for all the components to consider any cost
326 reductions over the model period, with intermediate values obtained through interpolation.
327 As suggested by Cole *et al.* [42], the cost of the battery component was divided into

328 power- and energy-related contributions. Cost projections of the PEM electrolyser and
 329 PEM fuel cell were taken from [43]. It was assumed that the ELY and FC stack
 330 replacements occur every 10 years [44]. The stack replacement cost was computed as a
 331 percentage of the CAPEX: 40% for ELY [43] and 50% for FC [45]. OPEX were assessed
 332 as a fraction of the CAPEX per year [46]. No cost evolution over time was considered for
 333 the hydrogen tank since the technology of steel pressure vessels is already mature [45].
 334 Finally, an annual discount rate equal to 4% was adopted in this analysis [46].

335 The charging and discharging efficiency of BATT was set to 95%. A value of 60%
 336 was assumed for the efficiency of the PEM electrolyser [46], while 51% was used for the
 337 efficiency of the PEM fuel cell [44]. An energy-to-power ratio range between 0.5 and 2
 338 was considered for the BATT component (Li-ion typology).

339

340 *Table 1 – Techno-economic assumptions (CAPEX and replacement) of components*
 341 *involved in the energy system.*

| | Capital cost (2021) | Capital cost (2030) | Capital cost (2040) | Operational life (years) | Ref. |
|-------------|--------------------------------|--------------------------------|--------------------------------|-------------------------------------|-------------|
| PV | 1022 k€/MW | 523 k€/MW | 405 k€/MW | 25 y | [47] |
| WT | 3705 k€/MW | 2181 k€/MW | 2025 k€/MW | 25 y | [48] |
| BATT | 500 k€/MW 154 k€/MWh | 332 k€/MW 102 k€/MWh | 304 k€/MW 89 k€/MWh | 10 y | [42,49] |
| ELY | 1300 k€/MW (40% stack) | 1000 k€/MW (40% stack) | 775 k€/MW (40% stack) | 20 y (stack: 10 y) | [43,44] |
| FC | 1520 k€/MW (50% stack) | 800 k€/MW (50% stack) | 650 k€/MW (50% stack) | 20 (stack: 10 y) | [43– 45] |
| HT | 15 k€/MWh | 15 k€/MWh | 15 k€/MWh | 20 | [50] |

342
 343 As shown in Table 2, each day was divided into 5 daily time brackets to consider the
 344 intraday variability of electricity consumption and renewable energy production. This
 345 detail on the daily variation (which was used for both the TRAD and NEW methods) is
 346 consistent with assumptions generally made in the literature for long-term energy
 347 expansion models [37]. The partitioning of days into time intervals is common in long-
 348 term energy models and is necessary to limit the computational cost and to ensure the
 349 solvability of the problem.

350
351

Table 2 – Daily time brackets in every representative day (for both TRAD and NEW methods).

| Daily time bracket | Start hour | End hour |
|--------------------|------------|----------|
| 1 | 0 | 6 |
| 2 | 6 | 10 |
| 3 | 10 | 14 |
| 4 | 14 | 18 |
| 5 | 18 | 24 |

352

353 The identification of the cost-optimal configuration of the energy system is allowed
354 from the first year (2021) onwards. The evolution of the energy system configuration over
355 the years is related to the increase in the total energy demand and to the cost-learning
356 curves of the involved components (see Table 1).

357 2.3 Scenario setting

358 The validation of the NEW method was done by performing a sensitivity analysis on the
359 number of representative days, which was increased up to 365. For the validation, the
360 energy simulation was performed over 1 year in order to solve the full time-scale model
361 (i.e., 365 representative days), which was used as a reference. The effectiveness of
362 TRAD as a function of the number of RDs was also analysed for comparison purposes.
363 In NEW, the required number of RDs was obtained by performing the clustering
364 procedure described in Section 2.1.2. In TRAD, the RDs were instead derived by
365 changing the number of *seasons* and considering a single *daytype* for each *season*. It
366 should be noted that the same number of RDs for TRAD and NEW also implies the same
367 number of *timeslices*.

368 For each case characterised by a certain number (*i*) of RDs, the relative error in the
369 objective function (i.e., the net present cost of the system) was evaluated as follows:

370

$$RE_{TRAD/NEW,i} = \frac{OF_{TRAD/NEW,i} - OF_{TRAD,365}}{OF_{TRAD,365}} \quad (2)$$

371

372 where $RE_{TRAD/NEW,i}$ is the relative error of the TRAD/NEW method with *i* RDs, and

373 $OF_{TRAD/NEW,i}$ is the objective function of the TRAD/NEW method with *i* RDs.

374 The goal of this sensitivity is to find the minimum number of RDs that can lead to an
375 accurate representation of the objective function and component sizes. This RD number
376 was then used to investigate the multi-year evolution of the Pantelleria energy system
377 (from year 2021 to year 2040). More specifically, different scenarios have been analysed
378 by varying the configuration of the EES system:

- 379 1. Only-battery scenario: the sizes of the hydrogen-based P2P components (ELY,
380 FC and HT) are set to zero.
- 381 2. Only-hydrogen scenario: the size of the battery is set to zero.
- 382 3. Hybrid scenario: no size constraints are set on the EES solutions (i.e., hydrogen
383 and batteries).

384 **3 Results and discussion**

385 Simulations were performed on a desktop computer with an Intel® Xeon® CPU
386 E3-1245 v5 @ 3.50GHz CPU and 32 GB RAM. The IBM ILOG® CPLEX® Optimization
387 Studio software was employed as solver of the MILP models, imposing a relative MIP gap
388 tolerance of 0.01%.

389 Representative days were introduced to reduce the complexity of the MILP-based
390 optimisation framework (Section 3.1). Their influence was assessed using a single-year
391 model to allow the resolution of the full-scale problem (with all 365 days of the year). The
392 aim was to identify a sufficiently accurate model to then address the design of multi-year
393 renewable energy systems (Section 3.2).

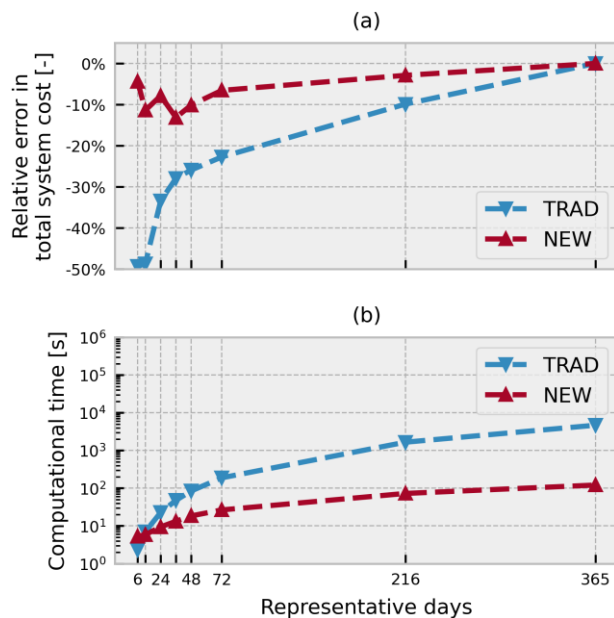
394 **3.1 Impact of representative days**

395 The energy system optimisation was run several times performing a sensitivity
396 analysis on the number of representative days: from 6 RDs up to the full-scale solution
397 (i.e., 365 RDs). The goal was to evaluate the minimum number of RDs needed to obtain
398 an accurate approximation of the full-scale objective function. Moreover, both NEW and
399 TRAD methods were applied to assess the effectiveness of interconnected clustered RDs
400 in the modelling of hydrogen-based EES systems. This analysis was performed on a
401 single year, using the electrical demand profiles and technology costs expected for the
402 year 2040.

403 The relative error of the objective function with respect to the full-scale model is
404 depicted in Figure 3a. It can be noted that the relative error of NEW is always lower than
405 that of TRAD, thus showing that the NEW approach provides better accuracy in

406 estimating the total system cost. When using very few representative days, from 6 to 12,
 407 the relative error of the traditional method is close to -50%. In contrast, the NEW
 408 technique can find an optimal system configuration with relative error of around 10%. For
 409 both methods, the objective function tends to converge by increasing the RD number until
 410 reaching the same value when 365 representative days are considered.

411 As displayed in Figure 3b, the use of RDs effectively reduces the computational
 412 burden of the problem. The computational time of the TRAD approach increases from 2.3
 413 s at 6 RDs to 4679 s at 365 RDs. Moreover, a 23-fold increase can be observed in the
 414 NEW approach when moving from 6 RDs to the full-scale solution. Although additional
 415 variables have been added in the NEW approach (related to the modelling of the storage
 416 component), the TRAD time curve is characterised by a greater slope. This can be due
 417 to an increase in the number of binary parameters needed to assign a certain *timeslice*
 418 to a *season* in the TRAD method [30].



419
 420 *Figure 3 - Relative error in total system cost (a) and computational time (b) for NEW and*
 421 *TRAD methods as a function of the number of representative days.*

422
 423 Main sizing outcomes as a function of the number of RDs are displayed in Figure
 424 4, where the dashed black lines refer to the full-scale solution. The rated power of the PV
 425 and WT technologies is well approximated over the entire RD interval for both the TRAD
 426 and NEW methods. The optimal PV size is always equal to 10.8 MW, which corresponds
 427 to the upper boundary of the PV size decision variable, as pointed out in Section 2.2.

428 Unlike the TRAD approach, the NEW technique can accurately evaluate the battery size,
429 i.e., rated power and energy, even when very few representative days are used. The
430 benefits of NEW are also evident in estimating the size of the hydrogen-based
431 components, i.e., electrolyser, fuel cell and hydrogen tank. The ELY and FC sizes quickly
432 converge close to the full-scale solution when the NEW approach is used. Compared to
433 TRAD, NEW also identifies a more accurate value of the HT rated energy in all the RD
434 configurations. As for the TRAD technique, the HT capacity is almost null in the range
435 from 6 to 12 RDs. The error on the HT capacity reaches -35% of the full-scale size when
436 using 24-48 RDs and then gradually improves to the full-scale solution. By contrast,
437 considering the NEW method, the underestimation of the HT rated energy is always less
438 than 12% from 12 RDs onwards. The use of interconnected clustered RDs (i.e., the NEW
439 approach) is thus effective in predicting the long-term storage capacity of the hydrogen
440 tank, whose optimal rated energy (1365 MWh) is much higher than that of the battery
441 (1.73 MWh).

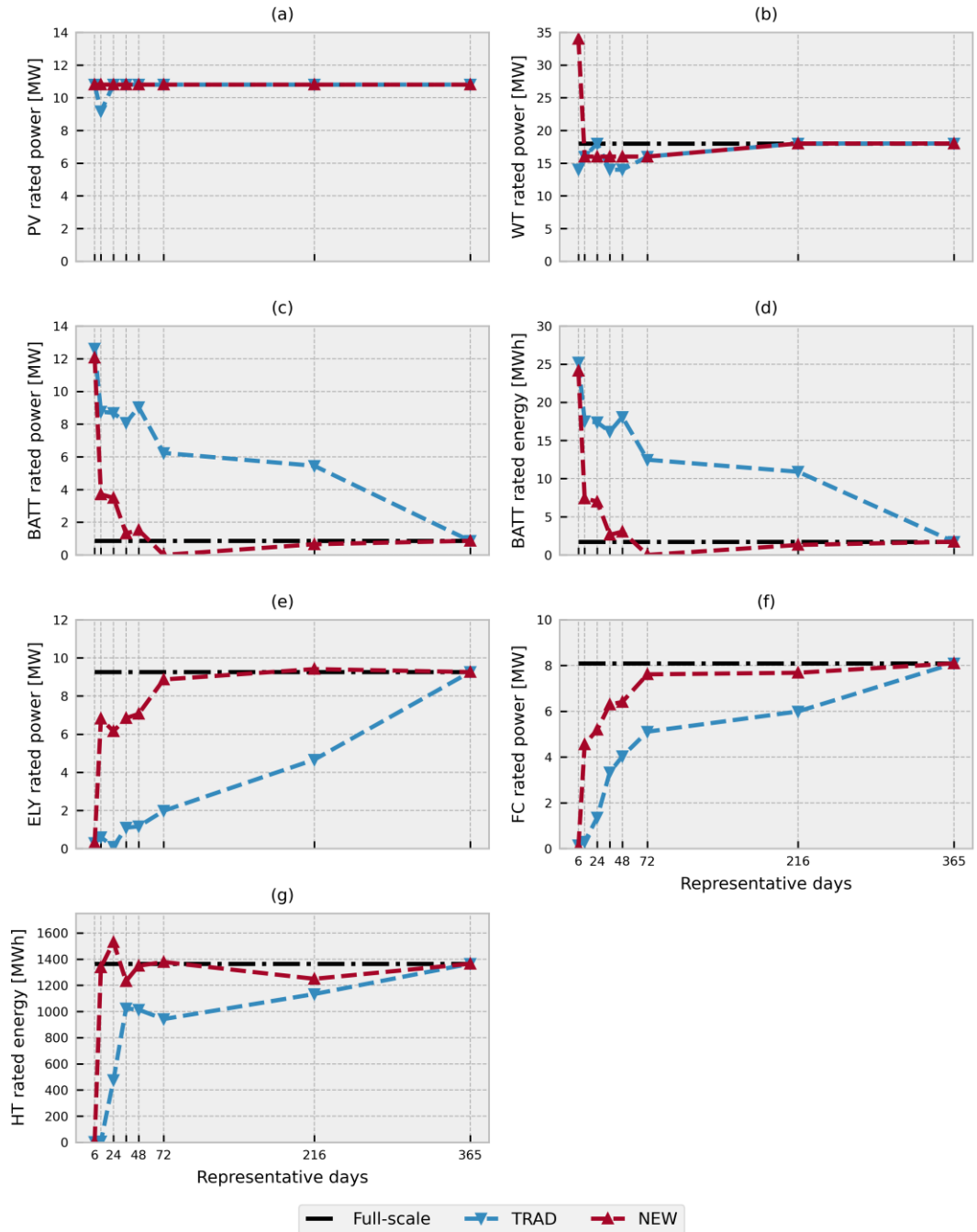
442 Overall, representative days have been demonstrated to reduce the required
443 simulation time while maintaining a good accuracy in the OF estimation. They were thus
444 employed for the development of the 20-year energy system model of Pantelleria island,
445 whose full-scale resolution is unfeasible with the available hardware.

446 It should be noted that the current work is mainly focused on validating the newly
447 introduced methodology in an energy system characterised by long-term energy storage
448 and on developing a comparative discussion about the functionality of batteries and
449 hydrogen in a 100% renewable energy scenario. However, the obtained results show that
450 this methodology could also be extended to the modelling of more complex energy
451 systems, thanks to the reduced computational effort ensured by the use of time slices
452 and the improved reliability of the model.

453

454

455



456

457 *Figure 4 - PV rated power (a), WT rated power (b), BATT rated power (c), BATT rated*
 458 *energy (d), ELY rated power (e), FC rated power (f) and HT rated energy (g) in 2040 for TRAD*
 459 *and NEW methods as a function of the number of representative days. The full-scale solution*
 460 *refers to 365 representative days.*

461

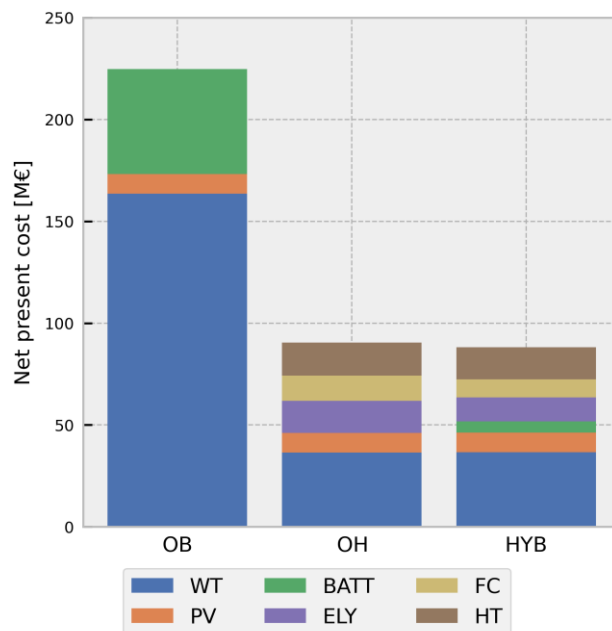
462 3.2 Scenarios comparative assessment

463 The multi-year energy model of Pantelleria, from 2021 to 2040, is here presented
 464 for the NEW approach and considering 48 RDs (240 *timeslices*), which were shown to

465 provide accurate sizing results (see Section 3.1). Three different scenarios have been
 466 investigated by varying the EES solution: only-battery (OB), only-hydrogen (OH) and
 467 hybrid (HYB) configurations.

468 The breakdown of the net present cost of the three scenarios is displayed in Figure
 469 5. The system configuration with hybrid storage is the most cost-effective solution with an
 470 NPC of 87.9 M€, followed by the only-hydrogen case, whose NPC is slightly higher (90.2
 471 M€). A 155% NPC increase can be observed when changing from the hybrid to the only-
 472 battery storage system (224.8 M€). As shown in Figure 5, approximately 70% of the OB
 473 cost is due to the wind farm subsystem. The battery storage also covers a relevant share
 474 of the cost (23%). It should be noted that the WT cost decreases significantly, by roughly
 475 4.5 times, when the hydrogen-based PtP solution is included in the energy system (i.e.,
 476 OH and HYB scenarios). The implementation of hydrogen storage is thus highly effective
 477 in limiting the costs when aiming at 100% renewable energy systems. In this case study,
 478 the PV cost share is the same for the three scenarios since the optimal PV rated power
 479 is always equal to the maximum installable PV power, i.e., 10.8 MW.

480



481

482
 483

Figure 5 - Breakdown of the net present cost (over 20 years project lifetime) in the only-battery (OB), only-hydrogen (OH) and hybrid (HYB) scenarios.

484

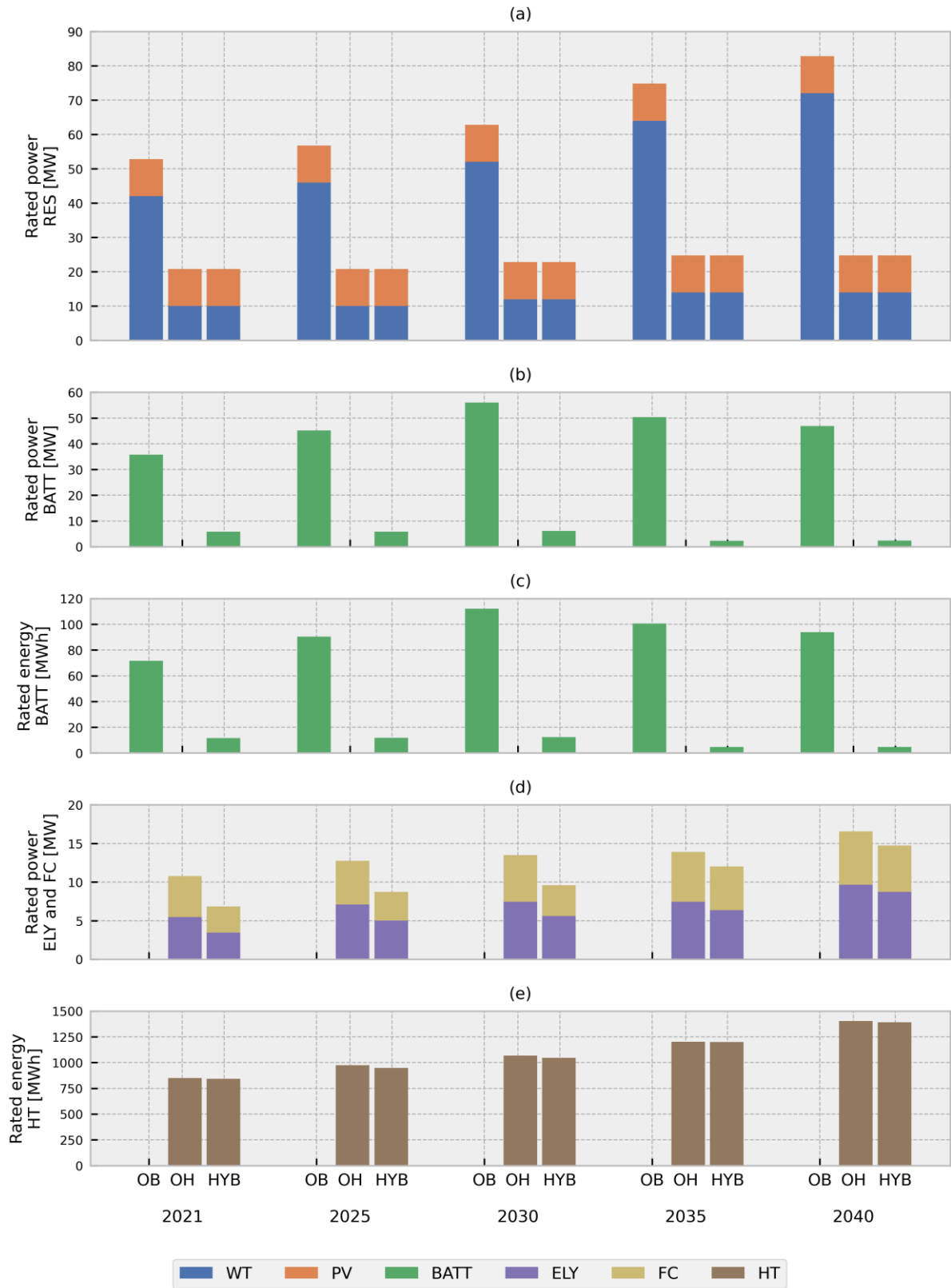
485 The main sizing results over the selected time horizon are reported in Figure 6 for
486 the OB, OH and HYB scenarios. The corresponding sizing values are specified in the
487 Appendix, Table A.1.

488 As shown in Figure 6a, in the only-battery scenario, the WT size increases from
489 42 MW in 2021 to 72 MW in 2040 to cope with the increase in load over years on the
490 island of Pantelleria. The large WT size of the OB scenario is also accompanied by a
491 high-capacity battery, whose rated power and energy (in the year 2040) are 46.9 MW and
492 93.8 MWh, respectively (i.e., energy to power ratio of 2 hours). It can be noted that, in the
493 OB scenario, the installed battery size has a maximum value in the year 2030 (Figure 6b
494 and c). From 2030 onwards, the increase in the annual electrical demand is thus mainly
495 addressed by increasing the WT rated power installed per year, which turns out to be a
496 cost-optimal planning strategy according to the cost projections reported in Table 1.

497 At the beginning of the project period, the OH and HYB cases require a WT size
498 of 10 MW, which is about 4 times smaller than that needed in the OB scenario (Figure
499 6a). However, large-size hydrogen storage is computed for the OH and HYB scenarios,
500 from 842-851 MWh in 2021 to 1391-1403 MWh in 2040 (Figure 6e). As previously shown
501 in Figure 5, the H₂-based power-to-power solution is essential in lowering the cost of the
502 energy system. In particular, the most cost-effective solution involves the presence of a
503 hybrid storage system that combines battery and hydrogen technologies. In the HYB
504 scenario, considering the year 2020, the rated energy of the battery is 73 times smaller
505 than that of the hydrogen tank (11.6 MWh of BATT compared to 842 MWh of HT). This
506 size discrepancy further increases over the years: in 2040, indeed, the rated energy of
507 BATT is 4.7 MWh, while 1391 MWh are foreseen for the HT. The adoption of batteries
508 has almost no impact on the long-term capacity of the hydrogen tank, which is roughly
509 the same in the OH and HYB scenarios. However, batteries in the HYB case are useful
510 to reduce the rated power of the ELY and FC components with respect to the OH case.
511 As displayed in Figure 6d, in 2021, the ELY size changes from 5.5 MW (OH) to 3.5 MW
512 (HYB) and the FC size changes from 5.3 MW (OH) to 3.4 MW (HYB). This is because the
513 short-term BATT storage intervenes in support of the H₂-based PtP to cover the electrical
514 demand peaks, thus avoiding oversizing the rated power of the hydrogen equipment.

515 It is also worth noting that, in the OH and HYB scenarios, the increase in the WT
516 rated power (from 10 MW in 2021 to 14 MW in 2040) is lower compared to the OB
517 scenario. It is, indeed, more convenient to invest in a greater hydrogen-based storage

518 (and, thus, improve the actual RES exploitation) rather than further increasing the size of
519 the wind farm. Moreover, it can be observed that the sizing results in 2040 for the multi-
520 year model differ slightly from the values of the single-year simulation with the same RD
521 number (see Section 3.1). This is because, in the multi-year approach, the sizing results
522 at the end of the simulation are influenced by the evolution of the energy system during
523 previous years.



524

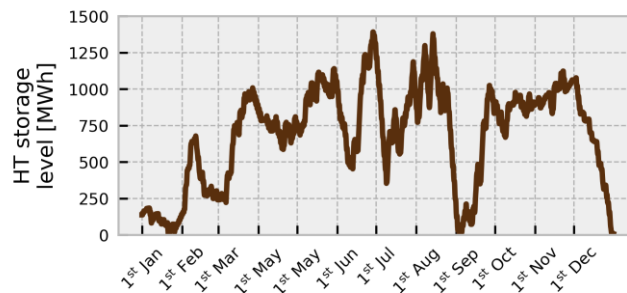
525

526

527

Figure 6 - Main sizing results in the only-battery (OB), only-hydrogen (OH) and hybrid (HYB) scenarios: rated power of PV and WT (a); rated power of BATT (b), rated energy of BATT (c), rated power of ELY and FC (d); and rated energy of HT (e).

528 Figure 7 shows the profile of the energy stored in the hydrogen tank expected for
529 the year 2040 in the HYB scenario. This trend is typical of a long-term storage system:
530 the HT is filled during the first part of the year and then emptied during the summer
531 because of the higher electrical demand. Therefore, the HT function is essential to
532 maintain a reliable electricity supply service throughout the entire year. On the contrary,
533 BATT acts as a short-term energy buffer, mainly supporting the hydrogen system during
534 peak demand.
535



536

537 *Figure 7 - Energy stored in the HT storage over the year (2040) in the HYB scenario.*

538
539 The average round-trip efficiency of the hydrogen-based PtP is 31%, i.e., 60% of
540 ELY efficiency multiplied by 51% of FC efficiency. This value is three times lower than the
541 average round-trip efficiency of the BATT-based PtP (90%), given by the product of the
542 BATT charging (95%) and discharging (95%) efficiencies. However, even if the hydrogen
543 route is much less efficient than the battery route, hydrogen was found to be crucial to
544 achieve a cost-optimal 100% renewable energy system. Due to the cost-effective long-
545 term storage capability of HTs, hydrogen makes it possible to better exploit local
546 renewable energy sources, thus avoiding a costly oversizing of the RES power plants.
547 On the island of Pantelleria, in 2021, the WT rated power is 10 MW in the HYB and OH
548 scenarios and 42 MW in the OB scenario, and this difference in size increases over the
549 years (14 MW compared to 72 MW in 2040).

550 It is also worth noting that, in the H₂-based PtP, the rated energy and power are
551 decoupled and belong to different components, which is a key feature in RES-based
552 applications when a long-duration EES system is required. In fact, as for the hybrid
553 scenario, in 2040 the rated power of ELY and FC is 8.7 MW and 6 MW, respectively;
554 whereas the rated energy of the hydrogen tank is around 1400 MWh, which is needed to

555 cope with the seasonal variation of the electrical demand in Pantelleria. On the contrary,
556 the rated energy-to-power ratio is constrained in the BATT solution and depends on the
557 BATT technology adopted. Finally, self-discharge losses, which were not implemented in
558 this analysis, would shift the results further in favour of hydrogen. They are, in fact, null
559 for the hydrogen storage but not negligible for the battery solution, especially when
560 dealing with high-capacity storage systems. However, as shown in the HYB scenario,
561 batteries are effective and still needed - due to their high efficiency and fast response - to
562 support the RES-based energy system in daily operation.

563 **4 Conclusions**

564 In this work, time series clustering was used to improve the modelling of energy systems
565 with a high share of renewable energy. Different EES configurations (i.e., only-battery,
566 only-hydrogen, and hybrid) were investigated to disclose the role of batteries and
567 hydrogen in 100% renewable-based systems. The main conclusions are summarised
568 below:

- 569 • The use of interconnected clustered representative days (NEW method) was
570 shown to be effective to address the modelling of energy systems with long-term
571 energy storage. Few representative days, from around 48, are needed to obtain
572 an accurate representation of the objective function (NPC) and the component
573 sizes. Due to the reduced computational effort, this method can be extended to
574 the modelling of more complex energy systems.
- 575 • Hydrogen storage plays a key role in achieving cost-effective system
576 configurations that rely entirely on local RESs. In the case study of Pantelleria, the
577 NPC of the only-battery energy system is 155% higher than that of the hybrid
578 (hydrogen + battery) alternative.
- 579 • In the HYB configuration, batteries assume anyway a useful role as short-term
580 energy buffer, supporting the energy system in daily operation and reducing the
581 installed rated power of the ELY and FC components.
- 582 • Although the hydrogen-based pathway is less efficient (about three times lower)
583 than the battery-based pathway, the advantage of hydrogen lies in the low-cost
584 high-capacity hydrogen tanks, which become crucial in RES-based energy
585 systems to address the seasonal behaviour of renewable production and electrical
586 demand. Long-term storage of hydrogen enhances the exploitation of renewable

587 energy, avoiding costly oversizing of renewable generators. As an example, in
588 2040 the WT rated power in the hydrogen-based scenarios (i.e., OH and HYB) is
589 around 5 times lower than that needed in the OB scenario.

590 Based on the methodology proposed in this work, future steps will address the
591 development of a spatially resolved model of the Pantelleria energy system, considering
592 a multi-nodal approach for a more accurate assessment of RES production across the
593 island. The impact of intraday variability on sizing results deserves also to be investigated
594 in future works.

595 **Abbreviations and acronyms**

| | |
|-------|----------------------------------|
| BATT | Battery |
| CAPEX | Capital Expenditures |
| DG | Diesel Generator |
| EES | Electrical Energy Storage |
| ELY | Electrolyser |
| FC | Fuel Cell |
| HRES | Hybrid Renewable Energy System |
| HT | Hydrogen Tank |
| HYB | Hybrid |
| LP | Linear Programming |
| MILP | Mixed Integer Linear Programming |
| NPC | Net Present Cost |
| OB | Only-Battery |
| OF | Objective Function |
| OH | Only-Hydrogen |
| OPEX | Operating Expenditures |
| PEM | Proton-Exchange Membrane |
| PtP | Power-to-Power |

| | |
|------|-------------------------|
| PtX | Power-to-X |
| PV | Photovoltaic |
| RD | Representative Day |
| RES | Renewable Energy Source |
| TRAD | Traditional |
| WT | Wind Turbine |

596

597 Appendix

598 Main sizing results of the 3 scenarios (OB, OH and HYB) are listed in Table A.1
 599 for the years 2021, 2030 and 2040.

600

601 *Table A.1 - Main sizing results in the only-battery (OB), only-hydrogen (OH) and hybrid*
 602 *(HYB) scenarios in 2021, 2030 and 2040 years.*

| Scenarios | | WT | PV | BATT | BATT | ELY | FC | HT |
|-----------|-----|------|------|------|-------|------|------|--------|
| | | [MW] | [MW] | [MW] | [MWh] | [MW] | [MW] | [MWh] |
| 2021 | OB | 42 | 10.8 | 35.8 | 71.6 | - | - | - |
| | OH | 10 | 10.8 | - | - | 5.5 | 5.3 | 850.9 |
| | HYB | 10 | 10.8 | 5.8 | 11.6 | 3.5 | 3.4 | 842 |
| 2030 | OB | 52 | 10.8 | 56 | 112.1 | - | - | - |
| | OH | 12 | 10.8 | - | - | 7.4 | 6 | 1067.7 |
| | HYB | 12 | 10.8 | 6.1 | 12.3 | 5.6 | 4 | 1047.4 |
| 2040 | OB | 72 | 10.8 | 46.9 | 93.8 | - | - | - |
| | OH | 14 | 10.8 | - | - | 9.7 | 6.9 | 1403 |
| | HYB | 14 | 10.8 | 2.4 | 4.7 | 8.7 | 6 | 1391.3 |

603

604

605 References

606 [1] International Electrotechnical Commission, Electrical Energy Storage - white paper,
 607 2019. <https://www.iec.ch/basecamp/electrical-energy-storage>.

- 608 [2] X. Luo, J. Wang, M. Dooner, J. Clarke, Overview of current development in
609 electrical energy storage technologies and the application potential in power
610 system operation, *Appl. Energy.* 137 (2015) 511–536.
611 <https://doi.org/10.1016/j.apenergy.2014.09.081>.
- 612 [3] H.C. Hesse, M. Schimpe, D. Kucevic, A. Jossen, Lithium-ion battery storage for the
613 grid - A review of stationary battery storage system design tailored for applications
614 in modern power grids, 2017. <https://doi.org/10.3390/en10122107>.
- 615 [4] S. Dutta, A review on production , storage of hydrogen and its utilization as an
616 energy resource, *J. Ind. Eng. Chem.* 20 (2014) 1148–1156.
617 <https://doi.org/10.1016/j.jiec.2013.07.037>.
- 618 [5] Z. Abdin, A. Zafaranloo, A. Rafiee, W. Mérida, W. Lipiński, K.R. Khalilpour,
619 Hydrogen as an energy vector, *Renew. Sustain. Energy Rev.* 120 (2020).
620 <https://doi.org/10.1016/j.rser.2019.109620>.
- 621 [6] G. Buffo, P. Marocco, D. Ferrero, A. Lanzini, M. Santarelli, Power-to-X and power-
622 to-power routes, in: *Sol. Hydrog. Prod.*, 2019: pp. 529–557.
623 <https://doi.org/10.1016/B978-0-12-814853-2.00015-1>.
- 624 [7] H. Lund, P.A. Østergaard, D. Connolly, B.V. Mathiesen, Smart energy and smart
625 energy systems, *Energy.* 137 (2017) 556–565.
626 <https://doi.org/10.1016/j.energy.2017.05.123>.
- 627 [8] H. Lund, J.Z. Thellufsen, P. Sorknæs, B.V. Mathiesen, M. Chang, P.T. Madsen,
628 M.S. Kany, I.R. Skov, Smart energy Denmark. A consistent and detailed strategy
629 for a fully decarbonized society, *Renew. Sustain. Energy Rev.* 168 (2022).
630 <https://doi.org/10.1016/j.rser.2022.112777>.
- 631 [9] H. Lund, P.A. Østergaard, D. Connolly, I. Ridjan, B.V. Mathiesen, F. Hvelplund, J.Z.
632 Thellufsen, P. Sorknses, Energy storage and smart energy systems, *Int. J. Sustain.*
633 *Energy Plan. Manag.* 11 (2016) 3–14. <https://doi.org/10.5278/ijsepm.2016.11.2>.
- 634 [10] D. Bionaz, P. Marocco, D. Ferrero, K. Sundseth, M. Santarelli, Life cycle
635 environmental analysis of a hydrogen-based energy storage system for remote
636 applications, *Energy Reports.* 8 (2022) 5080–5092.
637 <https://doi.org/10.1016/j.egy.2022.03.181>.
- 638 [11] D. Haase, A. Maier, Islands of the European Union: State of play and future
639 challenges, 2021.
640 [26](https://www.europarl.europa.eu/RegData/etudes/STUD/2021/652239/IPOL_STU(</p></div><div data-bbox=)

- 641 2021)652239_EN.pdf.
- 642 [12] X. Qi, J. Wang, G. Królczyk, P. Gardoni, Z. Li, Sustainability analysis of a hybrid
643 renewable power system with battery storage for islands application, *J. Energy*
644 *Storage*. 50 (2022) 104682.
645 <https://doi.org/https://doi.org/10.1016/j.est.2022.104682>.
- 646 [13] S. Hajiaghasi, A. Salemnia, M. Hamzeh, Hybrid energy storage system for
647 microgrids applications: A review, *J. Energy Storage*. 21 (2019) 543–570.
648 <https://doi.org/https://doi.org/10.1016/j.est.2018.12.017>.
- 649 [14] R. Siddaiah, R.P. Saini, A review on planning, configurations, modeling and
650 optimization techniques of hybrid renewable energy systems for off grid
651 applications, *Renew. Sustain. Energy Rev.* 58 (2016) 376–396.
652 <https://doi.org/10.1016/j.rser.2015.12.281>.
- 653 [15] Y. Liu, S. Yu, Y. Zhu, D. Wang, J. Liu, Modeling, planning, application and
654 management of energy systems for isolated areas: A review, *Renew. Sustain.*
655 *Energy Rev.* 82 (2018) 460–470. <https://doi.org/10.1016/j.rser.2017.09.063>.
- 656 [16] M.G. Prina, V. Casalicchio, C. Kaldemeyer, G. Manzolini, D. Moser, A. Wanitschke,
657 W. Sparber, Multi-objective investment optimization for energy system models in
658 high temporal and spatial resolution, *Appl. Energy*. 264 (2020) 114728.
659 <https://doi.org/10.1016/j.apenergy.2020.114728>.
- 660 [17] O.D.T. Odou, R. Bhandari, R. Adamou, Hybrid off-grid renewable power system for
661 sustainable rural electrification in Benin, *Renew. Energy*. 145 (2020) 1266–1279.
662 <https://doi.org/10.1016/j.renene.2019.06.032>.
- 663 [18] P. Marocco, D. Ferrero, A. Lanzini, M. Santarelli, Optimal design of stand-alone
664 solutions based on RES + hydrogen storage feeding off-grid communities, *Energy*
665 *Convers. Manag.* 238 (2021) 114147.
666 <https://doi.org/10.1016/j.enconman.2021.114147>.
- 667 [19] H. Mun, B. Moon, S. Park, Y. Yoon, A study on the economic feasibility of stand-
668 alone microgrid for carbon-free island in Korea, *Energies*. 14 (2021).
669 <https://doi.org/10.3390/en14071913>.
- 670 [20] P. Marocco, D. Ferrero, A. Lanzini, M. Santarelli, The role of hydrogen in the optimal
671 design of off-grid hybrid renewable energy systems, *J. Energy Storage*. 46 (2022)
672 103893. <https://doi.org/10.1016/j.est.2021.103893>.
- 673 [21] M. Chang, J.Z. Thellufsen, B. Zakeri, B. Pickering, S. Pfenninger, H. Lund, P.A.

- 674 Østergaard, Trends in tools and approaches for modelling the energy transition,
675 Appl. Energy. 290 (2021). <https://doi.org/10.1016/j.apenergy.2021.116731>.
- 676 [22] C. Mokhtara, B. Negrou, A. Bouferrouk, Y. Yao, N. Settou, M. Ramadan, Integrated
677 supply–demand energy management for optimal design of off-grid hybrid
678 renewable energy systems for residential electrification in arid climates, Energy
679 Convers. Manag. 221 (2020) 113192.
680 <https://doi.org/10.1016/j.enconman.2020.113192>.
- 681 [23] S. Sinha, S.S. Chandel, Review of software tools for hybrid renewable energy
682 systems, Renew. Sustain. Energy Rev. 32 (2014) 192–205.
683 <https://doi.org/10.1016/j.rser.2014.01.035>.
- 684 [24] S. Mohseni, A.C. Brent, D. Burmester, A comparison of metaheuristics for the
685 optimal capacity planning of an isolated, battery-less, hydrogen-based micro-grid,
686 Appl. Energy. 259 (2020) 114224. <https://doi.org/10.1016/j.apenergy.2019.114224>.
- 687 [25] M.G. Prina, D. Groppi, B. Nastasi, D.A. Garcia, Bottom-up energy system models
688 applied to sustainable islands, Renew. Sustain. Energy Rev. 152 (2021) 111625.
689 <https://doi.org/10.1016/j.rser.2021.111625>.
- 690 [26] R. Loulou, G. Goldstein, A. Kanudia, U. Remme, Documentation for the TIMES
691 Model Part I: TIMES Concepts and Theory, 2016. [http://www.iea-](http://www.iea-etsap.org/web/Documentation.asp)
692 [etsap.org/web/Documentation.asp](http://www.iea-etsap.org/web/Documentation.asp) (accessed October 23, 2020).
- 693 [27] M. Howells, H. Rogner, N. Strachan, C. Heaps, H. Huntington, S. Kypreos, A.
694 Hughes, S. Silveira, J. DeCarolis, M. Bazillian, A. Roehrl, OSeMOSYS: The Open
695 Source Energy Modeling System. An introduction to its ethos, structure and
696 development, Energy Policy. 39 (2011) 5850–5870.
697 <https://doi.org/10.1016/j.enpol.2011.06.033>.
- 698 [28] R. Novo, F.D. Minuto, G. Bracco, G. Mattiazzo, R. Borchiellini, A. Lanzini,
699 Supporting Decarbonization Strategies of Local Energy Systems by De-Risking
700 Investments in Renewables: A Case Study on Pantelleria Island, Energies. 15
701 (2022). <https://doi.org/10.3390/en15031103>.
- 702 [29] L. Kotzur, P. Markewitz, M. Robinius, D. Stolten, Time series aggregation for energy
703 system design: Modeling seasonal storage, Appl. Energy. 213 (2018) 123–135.
704 <https://doi.org/10.1016/j.apenergy.2018.01.023>.
- 705 [30] R. Novo, P. Marocco, G. Giorgi, A. Lanzini, M. Santarelli, G. Mattiazzo, Planning
706 the decarbonisation of energy systems: the importance of applying time series

- 707 clustering to long-term models, *Energy Convers. Manag.* X. 15 (2022) 100274.
708 <https://doi.org/https://doi.org/10.1016/j.ecmx.2022.100274>.
- 709 [31] P. Gabrielli, M. Gazzani, E. Martelli, M. Mazzotti, Optimal design of multi-energy
710 systems with seasonal storage, *Appl. Energy.* 219 (2018) 408–424.
711 <https://doi.org/10.1016/j.apenergy.2017.07.142>.
- 712 [32] L. Kotzur, P. Markewitz, M. Robinius, D. Stolten, Impact of different time series
713 aggregation methods on optimal energy system design, *Renew. Energy.* 117
714 (2018) 474–487. <https://doi.org/10.1016/j.renene.2017.10.017>.
- 715 [33] M. Hoffmann, J. Priesmann, L. Nolting, A. Praktiknjo, L. Kotzur, D. Stolten, Typical
716 periods or typical time steps? A multi-model analysis to determine the optimal
717 temporal aggregation for energy system models, *Appl. Energy.* 304 (2021) 117825.
718 <https://doi.org/https://doi.org/10.1016/j.apenergy.2021.117825>.
- 719 [34] OSeMOSYS Community, GitHub OSeMOSYS Pyomo, (2022).
720 https://github.com/OSeMOSYS/OSeMOSYS_Pyomo (accessed November 26,
721 2022).
- 722 [35] KTH Royal Institute of Technology - School of Industrial Engineering and
723 Management division of Energy Systems Analysis, KTH Royal Institute of
724 Technology, OSeMOSYS Documentation, 2019.
- 725 [36] K. Poncelet, E. Delarue, D. Six, J. Duerinck, W. D’haeseleer, Impact of the level of
726 temporal and operational detail in energy-system planning models, *Appl. Energy.*
727 162 (2016) 631–643. <https://doi.org/10.1016/j.apenergy.2015.10.100>.
- 728 [37] O. Balyk, K.S. Andersen, S. Dockweiler, M. Gargiulo, K. Karlsson, R. Næraa, S.
729 Petrović, J. Tattini, L.B. Termansen, G. Venturini, TIMES-DK: Technology-rich
730 multi-sectoral optimisation model of the Danish energy system, *Energy Strateg.*
731 *Rev.* 23 (2019) 13–22. <https://doi.org/10.1016/j.esr.2018.11.003>.
- 732 [38] M. Welsch, Enhancing the Treatment of Systems Integration in Long-term Energy
733 Models. Doctoral Thesis., 2013.
- 734 [39] GitHub - revised OSeMOSYS-Pyomo with new timeframe., (2022).
735 https://github.com/riccardonovo/OSeMOSYS_Pyomo/tree/OSeMOSYS_EC_2022
736 0118 (accessed November 26, 2022).
- 737 [40] G. Correa, P. Marocco, P. Muñoz, T. Falagüerra, D. Ferrero, M. Santarelli,
738 Pressurized PEM water electrolysis: Dynamic modelling focusing on the cathode
739 side, *Int. J. Hydrogen Energy.* 47 (2022) 4315–4327.

- 740 <https://doi.org/10.1016/j.ijhydene.2021.11.097>.
- 741 [41] Clean Energy for EU Islands, Energy Center Lab, Comune di Pantelleria, Parco
742 Nazionale Isola di Pantelleria, S.MED.E. Pantelleria S.p.A., SOFIP S.p.A., APS
743 Resilea, Cantina Basile, Agenda per la transizione energetica. Isola di Pantelleria,
744 2020. <https://clean-energy-islands.ec.europa.eu/countries/italy/pantelleria>.
- 745 [42] W. Cole, A.W. Frazier, C. Augustine, Cost Projections for Utility-Scale Battery
746 Storage: 2021 Update, 2021. <https://www.nrel.gov/docs/fy21osti/79236.pdf>.
- 747 [43] D. Thomas, D. Mertens, M. Meeus, W. Van der Laak, I. Francois, Power-to-gas
748 Roadmap for Flanders, Brussels, 2016.
749 [https://www.waterstofnet.eu/_asset/_public/powertogas/P2G-Roadmap-for-](https://www.waterstofnet.eu/_asset/_public/powertogas/P2G-Roadmap-for-Flanders.pdf)
750 [Flanders.pdf](https://www.waterstofnet.eu/_asset/_public/powertogas/P2G-Roadmap-for-Flanders.pdf).
- 751 [44] D.G. Caglayan, H.U. Heinrichs, M. Robinius, D. Stolten, Robust design of a future
752 100% renewable european energy supply system with hydrogen infrastructure, Int.
753 J. Hydrogen Energy. 46 (2021) 29376–29390.
754 <https://doi.org/10.1016/j.ijhydene.2020.12.197>.
- 755 [45] Tractebel, Inicio, Study on early business cases for H2 in energy storage and
756 more broadly power to H2 applications, 2017.
757 https://www.fch.europa.eu/sites/default/files/P2H_Full_Study_FCHJU.pdf.
- 758 [46] H. Böhm, A. Zauner, D.C. Rosenfeld, R. Tichler, Projecting cost development for
759 future large-scale power-to-gas implementations by scaling effects, Appl. Energy.
760 264 (2020). <https://doi.org/10.1016/j.apenergy.2020.114780>.
- 761 [47] International Renewable Energy Agency (IRENA), Future of solar photovoltaic.
762 Deployment, investment, technology, grid integration and socio-economic aspects,
763 2019. <https://www.irena.org/publications/2019/Nov/Future-of-Solar-Photovoltaic>.
- 764 [48] International Renewable Energy Agency (IRENA), Future of wind. Deployment,
765 investment, technology, grid integration and socio-economic aspects, 2019.
766 <https://www.irena.org/publications/2019/Oct/Future-of-wind>.
- 767 [49] E. Crespi, P. Colbertaldo, G. Guandalini, S. Campanari, Design of hybrid power-to-
768 power systems for continuous clean PV-based energy supply, Int. J. Hydrogen
769 Energy. 46 (2021) 13691–13708.
770 <https://doi.org/https://doi.org/10.1016/j.ijhydene.2020.09.152>.
- 771 [50] M. Reuß, T. Grube, M. Robinius, P. Preuster, P. Wasserscheid, D. Stolten,
772 Seasonal storage and alternative carriers: A flexible hydrogen supply chain model,

773 Appl. Energy. 200 (2017) 290–302.
774 <https://doi.org/10.1016/j.apenergy.2017.05.050>.
775